

Experiments at SMART and related activities

Hideyuki Sakai^{*1,*2}

The E4 experimental room is now occupied with the fixed-frequency Ring Cyclotron (fRC), a part of the RIBF accelerator complex. It was once occupied by the Swinger and Magnetic Analyzer with Rotator and Twister (SMART). SMART was a versatile magnetic spectrometer primarily designed for the spectroscopic study of nuclei by means of the missing-energy (mass) method induced by intermediate-energy heavy-ion beams ($A/Z \geq 2$) from the RIKEN Ring Cyclotron (RRC), and it was active during 1990–2005.

Here, some of the research programs conducted at SMART as well as related activities of the author's group are briefly described.

SMART magnetic spectrometer

The SMART magnetic spectrometer was designed and constructed by the SMART Group,¹⁾ led by Hajime Ohnuma of the Tokyo Institute of Technology.

SMART, shown in Fig. 1, consisted of a beam swinger and a magnetic spectrometer. To change the scattering angle of a reaction, the incident beam is swung with respect to the target, and the spectrometer stays still. The magnetic spectrometer was composed of three quadrupole magnets and two dipole magnets in the quadrupole-quadrupole-dipole-quadrupole-dipole (QQDQD) configuration.

The first three components (QQD) having the first focal plane FP1 were designed to work as a large-

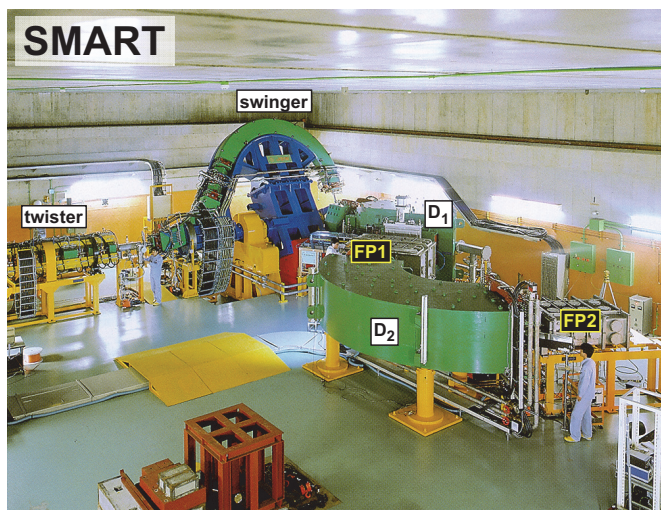


Fig. 1. Photograph of the SMART magnetic spectrometer in the E4 experimental hall.

^{*1} Senior Visiting Scientist from the University of Tokyo (1993–2010)

^{*2} At present RIKEN Nishina Center

solid-angle (20 msr) and wide-momentum-acceptance ($\delta p/p = 40\%$) spectrometer with a momentum resolution of $p/\Delta p = 4,000$. With the full configuration (QQDQD) having the second focal plane FP2, it works as a high-momentum-resolution ($p/\Delta p = 12,000$) spectrometer with a moderate solid angle (10 msr) and momentum acceptance ($\delta p/p = 4\%$).

The construction of SMART was finished in 1990, following which commissioning works were conducted. Regrettably, SMART was decommissioned in 2005 to create space to install fRC.

Construction of polarized ion source

Although the deuteron beam at the RIKEN Accelerator Research Facility (RARF) with a maximum energy of 270 MeV was already unique at the time, the author's group realized that it would become truly unique if the polarization degrees of freedom are available.

We proposed the construction of an atomic-beam-type Polarized Ion Source (PIS) dedicated to the deuteron beam in 1990 (Fig. 2). It was accepted by RARF. PIS construction was finished by 1992. The beam intensity achieved was about $140 \mu\text{A}$ with 80% polarization.²⁾ At the exit of PIS, a Wien filter system was equipped to rotate the deuteron polarization axis, i.e., the spin quantization axis. Owing to the single-

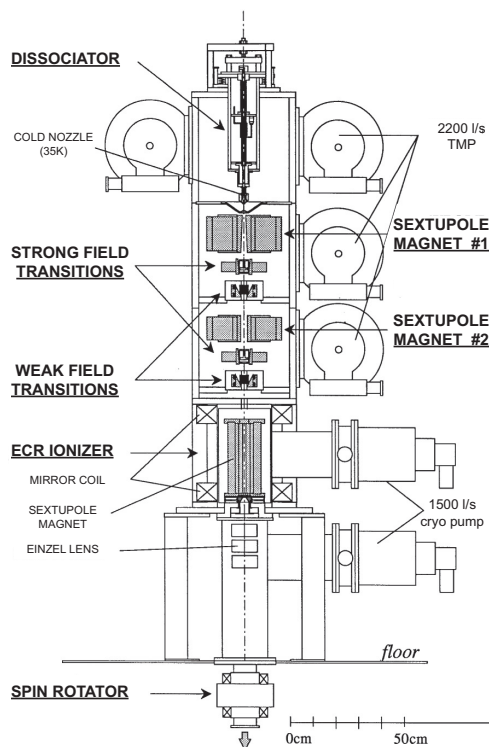


Fig. 2. Atomic-beam-type polarized ion source of RIKEN.

turn extraction for both the AVF injector cyclotron and RRC, the polarization axis is maintained during the accelerations, which allows us to control the polarization axis to any direction at the target position of SMART. This is the first facility in the world that realized this unique feature.

Polarization measurement with $d + p$ scattering

After the successful construction of PIS and subsequent acceleration of the polarized deuteron beam (\vec{d}) to 270 MeV, we needed to measure the absolute magnitude of the polarization. At the time, it was not known which reaction (scattering) should be chosen for polarimetry sensitive to both vector and tensor polarizations. Our first choice was the $\vec{d} + p$ scattering.

The complete analyzing powers ($A_y, A_{xx}, A_{yy}, A_{xz}$) for the elastic $\vec{d} + p$ scattering were successfully measured and published in Ref. [3] by using the beam-line polarimeter system together with the cross sections. Since all analyzing powers showed moderate magnitudes, it was concluded that the $\vec{d} + p$ scattering could be an ideal scattering reaction for polarimetry at

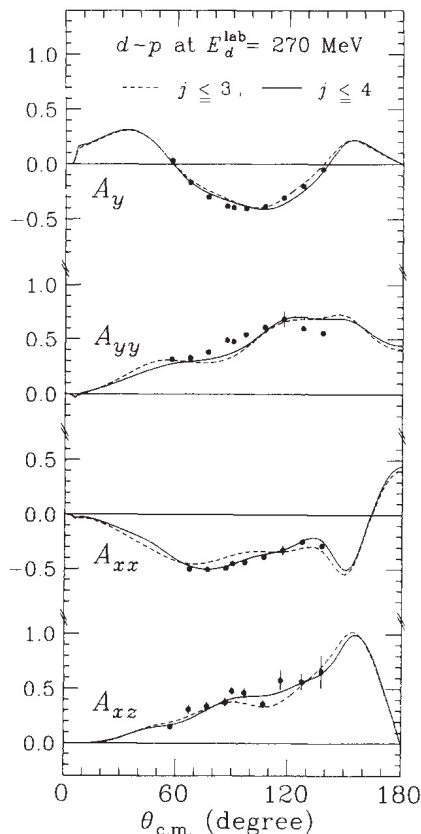


Fig. 3. Vector and tensor analyzing powers. Dashed and solid curves show the results of Faddeev calculations with the Argonne v_{14} 2NF for $j \leq 3$ and $j \leq 4$, respectively. See Ref. [3] for details.

270 MeV.

The measured results together with Faddeev-type three-body calculations employing the modern two-nucleon force (2NF) are shown in Fig. 4. A surprisingly large discrepancy of about 30% in the cross-section-minimum region of 100° – 150° was found between our measurement and the Faddeev calculations.

This discrepancy led us to get deeply involved in the study of the three-nucleon force (3NF).

Three-nucleon force study

Soon after the above study, the full Faddeev calculation with 2NF plus 3NF became available.⁴⁾ Meanwhile, we extended our $d + p$ scattering measurements to SMART, which allowed us to measure wide scattering angles $\theta_{c.m.} = 10^\circ - 180^\circ$. Moreover, the polarization transfer coefficients $K_{ij}^{y'}$ for the ${}^1\text{H}(\vec{d}, \vec{p})$ scattering were measured for the first time at $E_d = 270$ MeV. The scattered proton polarization was measured by the polarimeter (DPOL) set at FP2 of SMART. DPOL will be described later.

The results obtained at SMART were published in Ref. [5] together with the state-of-the-art Faddeev calculations with the modern 2NF + Tucson-Melbourne (TM) 3NF, as shown in Fig. 5 for cross sections and spin observables.

The cross-section difference is beautifully explained by the calculation, which is the first confirmation of the 3NF effects in the three-nucleon continuum (scattering) system. This was the milestone of the 3NF study. In contrast, some polarization observables were not described well with calculations, which indicates some deficiencies in the spin-dependent part of 3NF.

After this study, 3NF effects have been seriously considered not only in few-body systems but also in nuclear-structure calculations particularly for neutron-rich nuclei as well as for high-density matter such as a neutron star. For example, for the nuclear structure

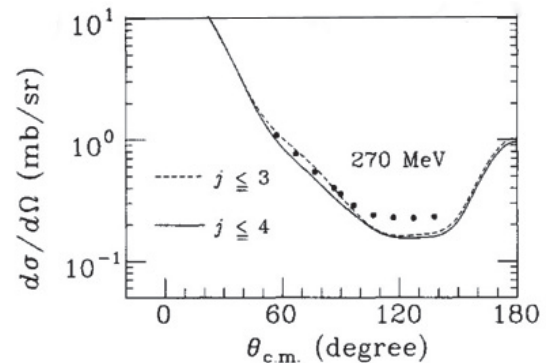


Fig. 4. Differential cross sections. The figure is taken from Ref. [3] with modification. The dashed and solid curves are the same as in Fig. 3.

calculation for neutron-rich Ca isotopes, see Ref. [6].

In SMART, measurements were extensively extended for the study of 3NF:

- Complete $d\sigma/d\Omega$, A_y^d , A_{xx} , A_{yy} , A_{xz} at $E(\vec{d}) = 140, 200,$ and 270 MeV.⁷⁾
- Polarization transfer $K_y^{y'}$, $K_{xx}^{y'}$, $K_{yy}^{y'}$, $K_{xz}^{y'}$, $P^{y'}$ for $\theta_{c.m.} = 90^\circ\text{--}180^\circ$ at $E(\vec{d}) = 270$ MeV.⁸⁾
- Resolving the $d\sigma/d\Omega$ discrepancy at $E(\vec{d}) = 270$ MeV.⁹⁾
- Polarization transfer for the breakup process of $\vec{d} + p \rightarrow \vec{p} + p + n$ at $E(\vec{d}) = 270$ MeV.¹⁰⁾

Now this comprehensive data-set has become a world standard for theoretical studies of 3NF effects.

The 3NF study was further extended to higher deuteron energies at the RIBF by constructing the BigDpol polarimeter:

- Complete A_y^d , A_{xx} , A_{yy} , A_{xz} at $E(\vec{d}) = 500$ and 596 MeV¹¹⁾ and at $E(\vec{d}) = 380$ MeV.¹²⁾

A four-body system was also studied by the ${}^2\text{H}({}^2\vec{\text{H}}, {}^3\text{He})n$ and ${}^2\text{H}({}^2\vec{\text{H}}, {}^3\text{H})p$ reactions at $E_d = 140, 200,$ and 270 MeV for wide scattering angles $\theta_{c.m.} = 0^\circ\text{--}110^\circ$. The physics interest here was that the tensor analyzing powers A_{xx} , A_{yy} , and A_{xz} could be sensitive to the D-state ($L = 2$) property in ${}^3\text{He}/{}^3\text{H}$. Ambiguity in the reaction mechanism prevented us from drawing a clear conclusion.^{13,14)}

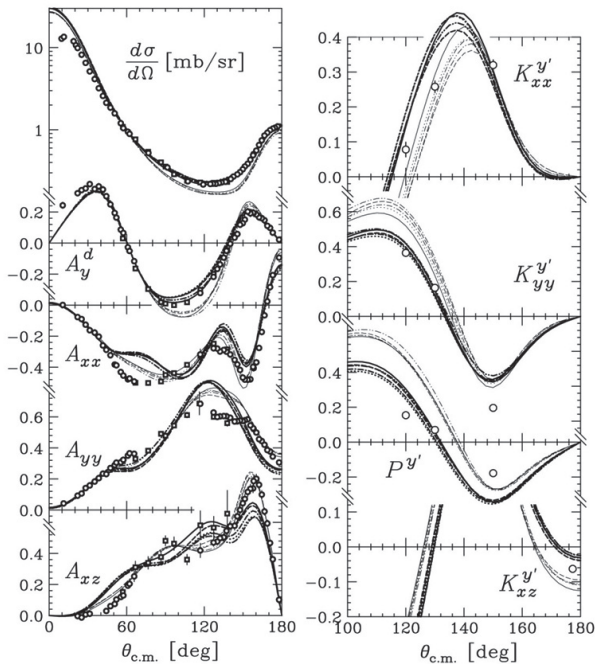


Fig. 5. Angular distributions of cross section, analyzing powers, and polarization transfer coefficients. See Ref. [5] for symbols and theoretical curves.

Spin-isospin responses with $(\vec{d}, {}^2\text{He})$ reaction

The $(d, {}^2\text{He})$ reaction has a very interesting quantum selection rule as a reaction probe. It excites exclusively spin-isospin flipped states $\Delta T = 1$ and $\Delta S = 1$, while the (n, p) reaction excites, in principle, $\Delta T = 1$ and $\Delta S = 1$ and 0. Thus, the $(\vec{d}, {}^2\text{He})$ reaction is suited for the study of the Gamow-Teller (GT) state 1^+ as well as spin-dipole states 0^- , 1^- , and 2^- starting from a 0^+ target. Those transitions are in the β^+ direction, which plays in some cases an essential role in the evolution of star burning or supernova explosion processes. Here, ${}^2\text{He}$ indicates the two-proton coupling to form the spin-singlet state $[{}^1\text{S}_0]$. To ensure $[{}^1\text{S}_0]$ experimentally, one needs to detect two protons in a small momentum corn ($\vec{p}_1 \simeq \vec{p}_2$), resulting in a small relative energy ($\epsilon < 1$ MeV). These conditions are not necessarily simple to satisfy by experimentally at an intermediate energy. The detection system for ${}^2\text{He}$ was constructed at FP1 of SMART.¹⁵⁾ The first results without polarization degrees of freedom were published in Refs. [16,17] to show the usefulness of the $(d, {}^2\text{He})$ reaction as a spectroscopic tool for GT transitions.

The tensor analyzing powers A_{xx} and/or A_{yy} of the

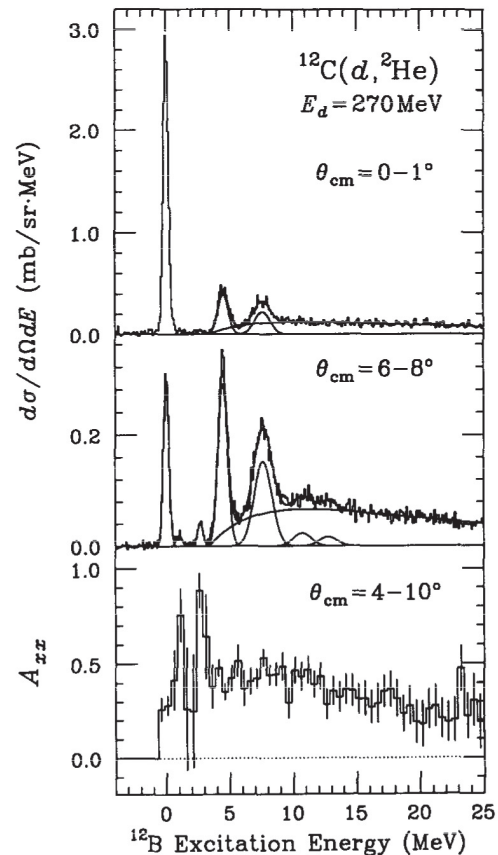


Fig. 6. Excitation energy spectra of cross section and A_{xx} . The figure is taken from Ref. [18].

($\vec{d}, {}^2\text{He}$) reaction are very useful as a spectroscopic tool in identifying the spin-parity J^π , in particular, for the spin-dipole states ($J^\pi = 0^-, 1^-, 2^-$). Finding a possible collective enhancement of 0^- states through its coupling to the pionic degrees of freedom in nuclei was of particular interest.

For natural-parity states, the tensor analyzing power predicted with PWIA tends to have an extreme value of

$$A_{xx} \sim +1 \quad \text{for } 1^- \text{ or } 2^+,$$

while that for the unnatural-parity 0^- state is

$$\left. \begin{array}{l} A_{xx} \sim -2 \\ A_{yy} = +1 \end{array} \right\} \text{ for } 0^-,$$

for the scattering angles in which the cross section becomes maximum. Note that the tensor analyzing power can take a value $+1 \geq A_{ij} \geq -2$.

At $\theta = 0^\circ$, A_{zz} takes an extreme value,

$$\begin{aligned} A_{zz}(0^\circ) &= +1 \quad \text{for } 1^- \text{ or } 2^+, \\ A_{zz}(0^\circ) &= -2 \quad \text{for } 0^-. \end{aligned}$$

Note that $A_{xx} = A_{yy}$ at $\theta = 0^\circ$ and $A_{xx} + A_{yy} + A_{zz} = 0$. It should be remarked that the result of $A_{zz}(0^\circ) = -2$ for 0^- is a model-independent one owing to the parity conservation in the spin-parity structure of $1^+ + 0^+ \rightarrow 0^+ + 0^-$.

The usefulness of the tensor analyzing powers was, for the first time, demonstrated by the ${}^{12}\text{C}(\vec{d}, {}^2\text{He}){}^{12}\text{B}$ reaction at $E_d = 270$ MeV.¹⁸⁾ The result is shown in Fig. 6.

A striking feature is the conspicuously large A_{xx} observed at energies corresponding to 2_1^+ (0.95 MeV) and 1_1^- (2.62 MeV), which agrees with the simple prediction above that A_{xx} becomes close to +1 for natural-parity states. The bump at $E_x = 7.5$ MeV in residual ${}^{12}\text{B}$ has been believed on the basis of many theoretical calculations and studies of (p, n) reactions to be dominated by 1^- states. However, the A_{xx} values corresponding to the bump are found to be almost similar to that of 2_2^- (4.5 MeV), which clearly indicates that the bump is dominated by 2^- .

A spectroscopic study on the neutron-rich light nuclei ${}^6\text{He}$, ${}^9\text{Li}$, and ${}^{11}\text{Be}$ was also performed.^{20,21)}

A model-independent spin-parity determination of the 0^- state was applied for the first time to the ${}^{12}\text{C}(\vec{d}, {}^2\text{He}){}^{12}\text{B}$ reaction by measuring the tensor analyzing power A_{zz} at $\theta = 0^\circ$.¹⁹⁾ The measurement was performed by preparing the tensor polarized deuteron beam aligned to the beam direction (p_{zz} beam), and the result is shown in Fig. 7.

It is indeed very remarkable to find that the A_{zz} of the peak at $E_x = 9.3$ MeV takes a very large negative value of ~ -1.2 . Thus, it is unambiguously concluded that the bump at 9.3 MeV is dominated by 0^- states. It is noted that $A_{zz} = -2$ holds only at exactly $\theta = 0^\circ$.

At $\theta \sim 5^\circ$, it takes another extreme value of $A_{zz} \sim +1$, demonstrating very strong angular dependence. The present experimental A_{zz} value of the peak at $E_x = 9.3$ MeV is an angle-integrated value over $\theta_{\text{c.m.}} = 0^\circ - 1^\circ$ and, therefore, $A_{zz} \sim -1.2$ instead of -2 .

$\Delta S = 1$ and 2 excitations via (\vec{d}, \vec{d}') with DPOL

Isoscalar spinflip states ($T = 0, S = 1$) are least known because the effective interaction V_σ responsible for the excitation is weak and there is no good experimental means to isolate the state.

The deuteron inelastic scattering (d, d') is very attractive to explore the isoscalar spinflip states. Since the deuteron has an intrinsic spin of $S = 1$, the inelastic scattering could have single spinflip $\Delta S = 1$ and double spinflip $\Delta S = 2$ processes in addition to a strong non-spinflip $\Delta S = 0$ process. The $\Delta S = 1$ and $\Delta S = 2$ spinflip processes may be connected to the target spin excitations of S_1 and S_2 , respectively. They are expressed in terms of polarization observables as follows:

$$\begin{aligned} S_1 &= \frac{1}{9}(4 - P^{y'y'} - A_{yy} - 2K_{yy}^{y'y'}), \\ S_2 &= \frac{1}{18}(4 + 2P^{y'y'} + 2A_{yy} - 9K_y^{y'} + K_{yy}^{y'y'}), \end{aligned}$$

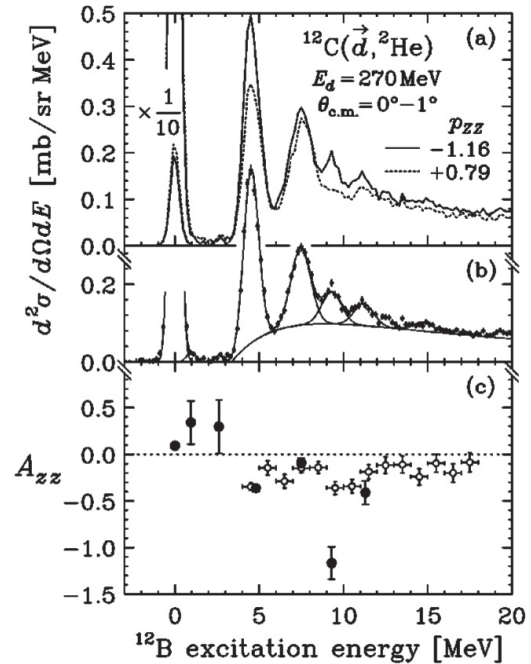


Fig. 7. (a) Double-differential cross sections at $\theta_{\text{c.m.}} = 0^\circ - 1^\circ$ as functions of ${}^{12}\text{B}$ excitation energy for $p_{zz} = -1.16$ and $+0.79$ polarized beams. (b) The result of peak fitting, and (c) the corresponding A_{zz} spectra. A_{zz} for each peak obtained by the fitting is shown by the closed circle, while that for the continuum binned in 1 MeV is shown by open circles. The figure is taken from Ref. [19].

where A , P , and K refer to the analyzing power, induced polarization, and polarization transfer coefficient, respectively. The vector and tensor polarizations of scattered deuterons have to be measured, which is experimentally very difficult and complicated. To measure S_1 and S_2 , we constructed the Deuteron Polarimeter (DPOL) at FP2 of SMART.²²⁾ DPOL utilizes the $\vec{d}+C$ elastic scattering and the $^1H(d, ^2He)$ reaction for vector and tensor polarization analysis, respectively.

The $^{12}C(\vec{d}, \vec{d}')$ reaction and $^{12}Si(\vec{d}, \vec{d}')$ reaction were measured and S_1 and S_2 were derived for the first time.^{22,23)} The result is shown in Fig. 8 for the cross section and the single- and double-spinflip cross sections. The S_1 value for the 2^+ state is close to zero, while that for the well-known 1^+ state at 12.71 MeV is large. This fact clearly indicates that S_1 will be an excellent spectroscopic tool to investigate isoscalar spin excitations.

It is quite surprising to find that the S_2 values are consistent with zero over the measured excitation energy region, and no clear indication of the double spin-flip ($\Delta S = 2$) state was found.

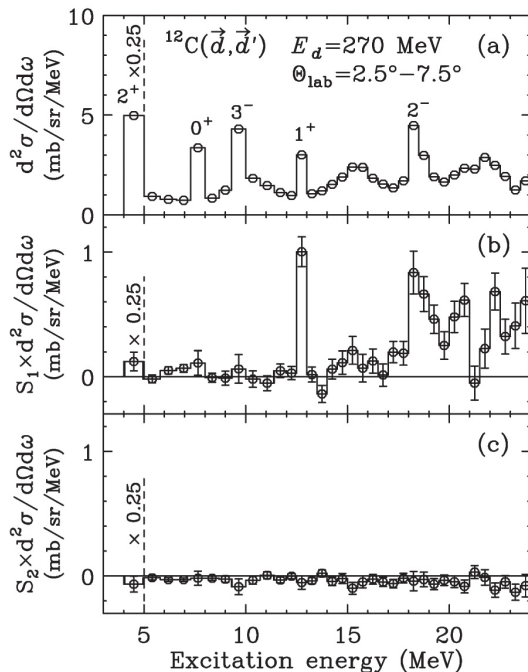


Fig. 8. Excitation energy spectra for the $^{12}C(d, d')$ reaction at $E_d = 270$ MeV integrated over $\theta_{lab} = 2.5^\circ - 7.5^\circ$. (a) An excitation energy spectrum. (b) The spectrum multiplied by S_1 . (c) The spectrum multiplied by S_2 . The figure is taken from Ref. [23].

HICEX reaction

Giant resonances represent major modes of collective motion of nuclei, and various multipole modes exist, reflecting isospin (T) and spin (S) degrees of freedom. Among them, an isovector non-spinflip quadrupole resonance (IVGQR), which is supposed to be a coherent state of $1p-1h$ excitations across two major shells ($2\hbar\omega$), was studied by the heavy-ion charge exchange reaction of $^{60}Ni(^{13}C, ^{13}N)^{60}Co$ at $E/A = 100$ MeV.²⁴⁾ The measurement was performed at the FP2 of SMART, where a pair of the cathode readout drift chambers²⁵⁾ was placed for ^{13}N detection.

Figure 9 shows typical energy spectra, which clearly display two prominent bumps at $E_x = 8.7 \pm 0.5$ MeV with $\Gamma = 2.8 \pm 0.8$ MeV and at $E_x = 20 \pm 2$ MeV with $\Gamma = 9 \pm 2$ MeV. To determine the multiplicities for those bumps, standard DWBA calculations were performed. The angular distributions of bumps were well fitted with the angular momentum transfers with $L = 1$ and $L = 2$, respectively. Based on this, it is concluded that the bump at $E_x = 8.7$ MeV is due to the well-known isovector giant dipole resonance (IVGDR) and the bump $E_x = 20$ MeV is due to IVGQR. Thus, IVGQR was unambiguously identified. It is interesting to note that an isovector giant monopole resonance (IVGMR), which is also expected at a $2\hbar\omega$ excitation energy and therefore should overlap with IVGQR, was not distinctly observed.

EPR paradox with EPOL

It is an intriguing and fascinating problem to verify the basic idea of quantum mechanics. It is well known that Einstein, Podolsky, and Rosen (EPR)²⁶⁾ asserted that quantum mechanics is incomplete in terms of lo-

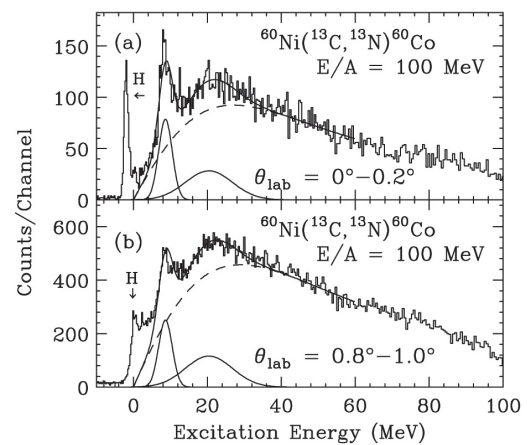


Fig. 9. Energy spectra of the $^{60}Ni(^{13}C, ^{13}N)^{60}Co$ reaction for the angular bins of (a) $\theta_{lab} = 0^\circ - 0.2^\circ$ and (b) $\theta_{lab} = 0.8^\circ - 1.0^\circ$. The figure is taken from Ref. [24].

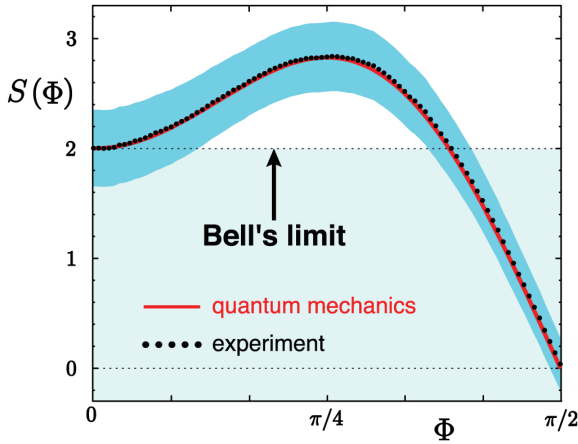


Fig. 10. Spin-correlation function $S(\Phi)$ vs Φ . The solid circles are experimental results compared with SHCH and quantum-mechanical predictions. Errors are shown by the blue band. The figure is taken from Ref. [30].

cal realism, a classical physicist's conception of nature. Bell²⁷⁾ rendered this argument quantitative and amenable to experimental verification, as he showed that any local hidden variable theory will result in an inequality, which can contradict quantum mechanical predictions, i.e., Bell's inequality or equivalently the Clauser, Horne, Shimony, and Holt (CHSH) inequality.²⁸⁾ The Bell-CHSH formulation concerns experiments where spin orientations have two possible outcomes (up/down). Many experiments have been performed with entangled photon pairs with great accuracy. However, there have not been any experiments with spin- $\frac{1}{2}$ particle pairs having mass with a statistically significant accuracy.

To conduct an experimental test of the Bell-CHSH inequality with massive particles, *viz.* two protons, two protons coupled to a spin singlet state [1S_0] as the initial state must be prepared, and the spin correlation of two separated protons satisfying the locality property in the final state must be measured. The two-proton system in the spin singlet state is nothing but ^2He , which is very familiar to us as an ejectile of the $(d, ^2\text{He})$ reaction. It should be mentioned especially that the use of ^2He has a huge merit. Since ^2He entangled by the strong interaction is an unbound two-proton system, two protons are automatically separated in a very gentle manner by the electromagnetic Coulomb force between them keeping their entanglement.

A spin polarimeter (EPOL) dedicated to measure the spins of two protons simultaneously was constructed and set up at FP2 of SMART.²⁹⁾

Entangled proton pairs were produced as a decay of ^2He formed in the $^1\text{H}(d, ^2\text{He})$ reaction at a 270 MeV deuteron beam. The experimental result is shown in Fig. 10.^{29,30)}

The quantum-mechanical prediction of the spin-correlation function is

$$S_{\text{QM}}(\Phi) = 3 \cos \Phi - \cos 3\Phi,$$

while that of Bell-CHSH states satisfied by local realistic theories is

$$S_{\text{CHSH}}(\Phi) \leq 2,$$

irrespective of Φ (opening angle between spins of a proton pair). For the definition of Φ , see Refs. [29,30]. It is amazing to find that the experimental data follow the quantum-mechanical prediction faithfully for the entire angular region and exceed Bell-CHSH's limit over a wide angular range.

At $\Phi = \pi/4$, the measured value of the spin-correlation function is

$$S_{\text{exp}}(\pi/4) = 2.83 \pm 0.24_{\text{sta}} \pm 0.07_{\text{sys}},$$

which violates Bell-CHSH inequality at the 99.3% confidence level. This is the first Bell-CHSH test using massive particles with significant accuracy. A characteristic feature of this experiment is that it is free from the loopholes of post-selection, causality (partially fulfilled), perfect detector efficiency (charged particle), and an 'event-ready' detection system.

Thus, EPR assertion does not seem to hold, and the 'Spooky action at distance,' phrased by Einstein against quantum-mechanical non-local phenomena, does exist.

Later, the Bell-CHSH inequality test was attempted with a proton-neutron pair in a singlet state via the $(d, pn[^1S_0])$ reaction. For that, a neutron polarimeter SMART-NPOL was constructed. Since the EPOL for proton and SMART-NPOL for neutron were separated by a few meters, a loophole of causality (space separation) could be overcome. Unfortunately, the statistical accuracy did not allow us to draw any conclusion.³¹⁾

Polarized ^3He target and $^3\vec{\text{He}}(\vec{d}, p)^4\text{He}$ reaction

The ground state of deuteron is a mixture of S- and D-states with orbital angular momenta of $L = 0$ and 2, respectively. Although the D-state plays an important role in determining various properties of the deuteron, it is not well determined, in particular at the high momentum region, owing to a lack of experimental means to directly access the D-state component.

A new approach to access the D-state component using the polarization correlation measurement by the $^3\vec{\text{He}}(\vec{d}, p)^4\text{He}$ reaction was proposed.³²⁾ The polarization correlation coefficient $C_{//}$ can be defined in terms of PWBA as

$$C_{//} = \frac{9}{4} \frac{w^2(k_{pn})}{u^2(k_{pn}) + w^2(k_{pn})}, \quad (1)$$

where $u^2(k_{pn})$ and $w^2(k_{pn})$ are the S- and D-state wave

functions of deuteron in momentum space, respectively, and k_{pn} is the internal momentum. It is remarkable to see that $C_{//}$ is directly proportional to $w^2(k_{pn})$.

The ${}^3\text{He}(\vec{d}, p){}^4\text{He}$ reaction was performed with the vector- and tensor-polarized deuteron beam of 270 MeV and a vector polarized ${}^3\text{He}$ target at $\theta_{\text{lab}} = 0^\circ$. For this purpose, a spin-exchange-type polarized ${}^3\text{He}$ gas target was constructed.³³⁾ The ${}^3\text{He}$ nuclei were polarized via the spin-exchange reaction with the optically pumped Rb atom. The ${}^3\text{He}$ gas density was 2.2×10^{20} atoms/cm³ with a polarization of 0.12. The result³²⁾ is shown in Fig. 11. Neither DWBA nor PWBA calculations could reproduce the present result, which cast a question on the relevance of the reaction mechanism.

Polarized proton target and ${}^6\text{He}(\vec{p}, p_0){}^6\text{He}$ scattering

It is quite exciting if we could extend spin-observable measurements to radio-isotope (RI) beams. In the RI experiments, a high-density target is necessary to gain sufficient luminosity since the intensity of the RI beams is typically less than 10^6 particles/s. In this respect, a solid target, rather than a gas target, is desirable. For the proton, a polarized solid proton target (PSPT) is available. However, a conventional PSPT system requires a high magnetic field (≥ 2.5 T) and a very low temperature (≤ 1 K), which is very inconvenient for the RI beam experiments because it inevitably utilizes inverse kinematics for the scattering, i.e., it is necessary to detect very-low-energy recoiling protons. We constructed a PSPT system that overcomes such experimental difficulties.

Since the construction of the PSPT system is described in Refs. [34,35] in detail, only an outline is given below. Protons in a single crystal of naphthalene (C_{10}H_8) doped with pentacene ($\text{C}_{22}\text{H}_{14}$) with a size of $4 \times 5 \times 2$ mm³ are polarized in a magnetic field of 0.3 T

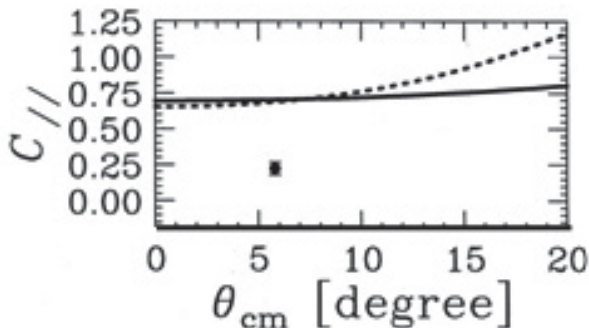


Fig. 11. Present datum in a black dot with statistical error. Solid and dashed lines are DWBA and PWBA calculations, respectively. The figure is taken from Ref. [32] with modification.

at 100 K by transferring a large population difference among the photo-excited triplet states of pentacene to the hydrogen nuclei. The proton polarization achieved was about 0.2.

The first RI beam experiment to measure the analyzing powers (A_y) for the ${}^6\text{He}(\vec{p}, p_{\text{gnd}}){}^6\text{He}$ scattering was conducted in inverse kinematics.³⁶⁾ The ${}^6\text{He}$ beam with 71 MeV/nucleon was provided by the RIKEN Projectile-fragment Separator (RIPS).

Figure 12 shows the first results, in which the analyzing powers are compared with those of ${}^6\text{Li}(\vec{p}, p_0){}^6\text{Li}$ scattering. Although the statistics are poor, the backward angular behavior of A_y seems to be very different from each other, even though the shapes of cross sections are similar. A very simple optical model analysis indicates that the spin-orbit potential for ${}^6\text{He}$ is located outside by about 0.8 fm compared to that for ${}^6\text{Li}$. It is noted that the present A_y behavior resembles that of the ${}^4\text{He}(\vec{p}, p_0){}^4\text{He}$ scattering.

Later, the ${}^6\text{He}(\vec{p}, p_0){}^6\text{He}$ scattering experiment was repeated with a higher proton polarization and improved detection system.³⁷⁾ Further, scattering from a more exotic nucleus ${}^8\text{He}(\vec{p}, p_0){}^8\text{He}$, was performed.³⁸⁾

Neutron radiology study

Radiological studies such as the neutron yield induced by heavy-ions³⁹⁾ or radioactive cross sections by

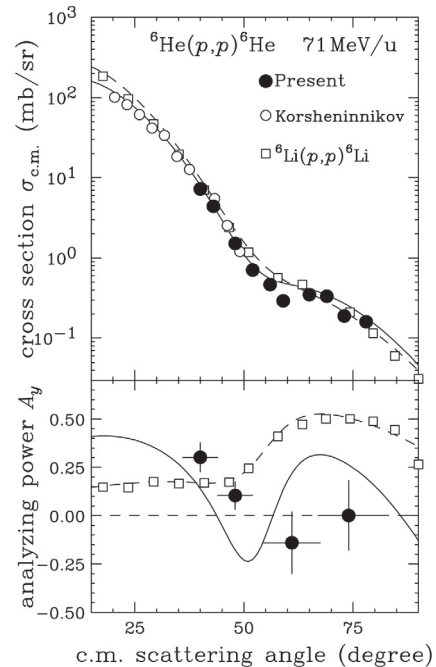


Fig. 12. Cross sections and analyzing powers. The solid and dashed lines are the results of optical model analyses fitted to the cross sections. The figure is taken from Ref. [36].

quasi-mono energetic neutrons^{40,41)} were conducted by Shouji Nakamura of Tohoku University and his collaborators using the swinger part of SMART. Obtained data provide very useful bases for designing radiation shields of accelerator facilities.

SHARAQ; successor of SMART

Although SMART was decommissioned and disassembled in 2005, its scientific motivation/tradition was partly succeeded by the SHARAQ project of the Center for Nuclear Study (CNS), the University of Tokyo. SHARAQ stands for Spectroscopy with High-resolution Analyzer of RadioActive Quantum beams.

The SHARAQ project was born while the author was the Director of CNS. The intention was to construct a high-resolution magnetic spectrometer dedicated to the RI beam experiments at RIBF. To achieve a high momentum resolution together with high angular resolution, SHARAQ was designed to have dispersion- and angular-matching functions utilizing the momentum dispersion of BigRIPS. The idea of ‘an exothermic charge-exchange reaction with unstable RI beams to explore exotic spin-isospin responses in nuclei with a magnetic spectrometer’ was approved by JSPS.⁴²⁾ The construction of SHARAQ started in 2005, and its commissioning started in 2010.

It should be mentioned that the first dipole magnet of SMART was reused in SHARAQ, again as the first dipole magnet in a QQDQD configuration. Thus, SHARAQ carried forward not only the scientific motivation but also a dipole magnet of SMART.

Summary and acknowledgments

In summary, various nuclear sciences were promoted exploiting the SMART magnetic spectrometer by many users. SMART was active for 15 years. During that period, 63 peer-reviewed papers were published, and 17 graduate students earned their Ph.D degrees.

Our group consistently pursued nuclear physics utilizing spin degrees of freedom of beam, target, and scattered particles. For that aim, we constructed PIS, DPOL, EPOL, SMART-NPOL, a polarized ³He target, and PSPT. Strong support by RARF is greatly appreciated, in particular on for PIS, the polarized ³He target, and PSPT constructions.

I am very much indebted to many collaborators and graduate students, who were the main contributors to the works mentioned above. Without their incessant hard working efforts of day and night, nothing could have been achieved. For lack of space, I regret that the names of contributors cannot be explicitly mentioned. However, I cannot help but mention my esteemed collaborator Hiroyuki Okamura (deceased). The construction of various devices and scientific works were the re-

sult of our cooperative but critical discussions. Without him, the scientific achievements described here could not be accomplished.

References

- 1) H. Ohnuma et al., Proc. Second IN2P3 RIKEN Symposium on Heavy-ion Collisions, edited by B. Heusch and M. Ishihara (World Scientific, Singapore, 1990), p. 26.
- 2) H. Okamura et al., AIP Conf. Proc. **293**, 84 (1994).
- 3) N. Sakamoto et al., Phys. Lett. B **367**, 60 (1996).
- 4) H. Witala et al., Phys. Rev. Lett. **81**, 1183 (1998).
- 5) H. Sakai et al., Phys. Rev. Lett. **84**, 5288 (2000).
- 6) T. Otsuka et al., Phys. Rev. Lett. **105**, 032501 (2010).
- 7) K. Sekiguchi et al., Phys. Rev. C **65**, 034003 (2002).
- 8) K. Sekiguchi et al., Phys. Rev. C **70**, 014001 (2004).
- 9) K. Sekiguchi et al., Phys. Rev. Lett. C **95**, 162301 (2005).
- 10) K. Sekiguchi et al., Phys. Rev. C **79**, 054008 (2009).
- 11) K. Sekiguchi et al., Phys. Rev. C **89**, 064007 (2014).
- 12) K. Sekiguchi et al., Phys. Rev. C, to be published.
- 13) T. Saito et al., Mod. Rhys. Lett. A **18**, 2 (2003).
- 14) V.P. Ladygin et al., Phys. Lett. B **598**, 47 (2004).
- 15) H. Okamura et al., Nucl. Instrum. Methods Phys. Res. A **406**, 78 (1998).
- 16) H. Ohnuma et al., Phys. Rev. C **93**, 648 (1993).
- 17) T. Niizeki et al., Nucl. Phys. A **577**, 37 (2009).
- 18) H. Okamura et al., Phys. Lett. B **345**, 1 (1995).
- 19) H. Okamura et al., Phys. Rev. C **66**, 054602 (2002).
- 20) T. Ohnishi, PhD thesis, The University of Tokyo, 2000.
- 21) T. Ohnishi et al., Nucl. Phys. A **687**, 38c (2001).
- 22) S. Ishida, PhD thesis, The University of Tokyo, 1998.
- 23) Y. Satou et al., Phys. Lett. B **521**, 153 (2001).
- 24) T. Ichihara et al., Phys. Rev. Lett. **89**, 142501 (2002).
- 25) M.H. Tanaka et al., Nucl. Instrum. Methods Phys. Res. A **362**, 521 (1995).
- 26) A. Einstein, B. Podolsky, N. Rosen, Phys. Rev. **47**, 777 (1935).
- 27) J. Bell, Physics **1**, 195 (1964).
- 28) J. F. Clauser, M. A. Horne, A. Shimony, R. A. Holt, Phys. Rev. Lett. **23**, 880 (1969).
- 29) T. Saito, PhD thesis, The University of Tokyo, 2005.
- 30) H. Sakai et al., Phys. Rev. Lett. **97**, 150405 (2006).
- 31) H. Kuboki, PhD thesis, The University of Tokyo, 2007.
- 32) T. Uesaka et al., Phys. Lett. B **467**, 199 (1999).
- 33) T. Uesaka et al., Nucl. Instrum. Methods Phys. Res. A **402**, 212 (1998).
- 34) M. Hatano, PhD thesis, The University of Tokyo, 2003.
- 35) T. Wakui et al., Nucl. Instrum. Methods Phys. Res. A **550**, 521 (2005).
- 36) M. Hatano et al., Euro. Phys. J. A **25**, 255 (2005).
- 37) T. Uesaka et al., Phys. Rev. C **82**, 021602(R) (2010).
- 38) S. Sakaguchi et al., Phys. Rev. C **87**, 021601(R) (2013).
- 39) H. Sato et al., Phys. Rev. C **64**, 033607 (2001).
- 40) N. Nakao et al., Nucl. Instrum. Methods Phys. Res. A **420**, 218 (1999).
- 41) E. Kim et al., Nucl. Sci. Eng. **129**, 209 (1998).
- 42) H. Sakai (Spokesperson), Grant-in-Aid for Specially Promoted Research 1700203.